Linear relaxation in large two-dimensional Ising models

Y. Lin and F. Wang[*]

Department of Physics, Xiamen University, Xiamen, Fujian 361005, China
(Received 19 December 2014; revised manuscript received 10 November 2015; published 8 February 2016; corrected 19 January 2018)

Critical dynamics in two-dimension Ising lattices up to 2048×2048 is simulated on field-programmable-gate-array- based computing devices. Linear relaxation times are measured from extremely long Monte Carlo simulations. The longest simulation has 7.1×10^{16} spin updates, which would take over 37 years to simulate on a general purpose computer. The linear relaxation time of the Ising lattices is found to follow the dynamic scaling law for correlation lengths as long as 2048. The dynamic exponent z of the system is found to be 2.179(12), which is consistent with previous studies of Ising lattices with shorter correlation lengths. It is also found that Monte Carlo simulations of critical dynamics in Ising lattices larger than 512×512 are very sensitive to the statistical correlations between pseudorandom numbers, making it even more difficult to study such large systems.

I. INTRODUCTION

Static critical phenomena have been well understood since Wilson's renormalization group (RG) breakthrough [1]; on the other hand, critical dynamics still attracts research attentions [2–9]. An understanding of the "critical slowing down" effect and accurate evaluation of the dynamic exponent z have been the focal point for many such studies. For a long time, linear relaxation simulations gave varied results on z due to insufficient data, limited by the extremely long simulation time [10–14]. Later on, methods based on nonequilibrium relaxation simulations were developed, and accurate evaluations of z around 2.167 were achieved with short simulation times [2,3,15–23]. Furthermore, the stochastic matrix method was utilized to calculate the relaxation times for small two-dimensional (2D) Ising lattices ($L \leqslant 16$) and z was found to be 2.167 as well [24,25]. The consolidation of the results from linear and nonlinear (nonequilibrium) simulations led to a consensus on the value of z. However, there are still reasons to pursue the subject further.

First of all, the correlation lengths of the Ising systems in these studies are all very short. The stochastic matrix-based linear relaxation study is only carried out to $L = 16$. The nonequilibrium studies are usually carried out in very large lattices, but the relevant correlation lengths are very short during the simulated initial relaxation process. Wang and Hu obtained a similar z of 2.168 from nonequilibrium relaxations in lattices less than 80×80 [21], indicating that the correlations' lengths involved in these nonequilibrium studies are probably not more than 100. It is therefore very meaningful to verify this result in finite size scaling (FSS) studies of Ising systems with longer correlation lengths.

Second, reasonable agreement between computer simulations and theoretical calculations has not been achieved. The high-temperature series-expansion method gives estimations between 2.0 and 2.3 [14,26–28], while the 4-ε expansion gives an estimation of 2.05 [4,5,29–32] and the $1 + \varepsilon$ gives an estimation of 2.50 [32]. Domany conjectured [33] that there is a dynamic critical point corresponding to the Lifshitz point for 2D Ising models, and a dynamic exponent z of 2.0 is derived rigorously from discrete dynamics based on certain cellular automation (CA) rules [34]. Since theoretical treatment of the critical dynamics generally involve Ising systems with infinitely long correlations lengths, one may wonder whether simulations of critical Ising systems with longer correlation lengths might reach agreement with one of these theoretical treatments.

Finally, nonasymptotic behaviors can usually be observed in critical phenomena as the system approaches its critical temperature and infinite correlation length [35–37]. It would be very interesting to see whether any such nonasymptotic behaviors can be observed in Ising systems approaching infinite size while maintaining critical temperature.

The main question that we would like to address in this paper is whether critical Ising systems with longer correlation lengths conform to the same dynamic exponent z value. We will answer this question by simulating linear relaxation processes in large 2D Ising models.

In linear relaxation studies, one can increase the correlation length of the Ising system by increasing the size of the Ising lattice. However, the "critical slowing down" effect puts strict limits on such efforts. To obtain adequate data, simulation time over 1000 times the relaxation time τ is needed for each data point, and as size L increases, τ increases even faster. The adequate computation time for simulating critical 2D Ising models scales to the $2 + z$ power of L. Computational resources can be dried up quickly by such an explosive scaling effect. No significant advancement has been reported since the few early studies that were carried out on the best vector supercomputers or special purpose computing machines at the time [13,38–41]. The reason for such stagnation in this pursuit, despite the tremendous progresses in high performance computing (HPC) technology, is due to the so-called "Von Neumann bottleneck" [42]. Monte Carlo simulations are communication-intensive computing tasks which have severe "Von Neumann bottleneck" latency problems on any central-processing-unit- based (CPU) computers while the advances in HPC have been mostly on cluster-based CPU platforms, which are an ill-fit for Monte Carlo simulations. The benchmarks left by the earlier studies are still not easy to beat on the current general purpose computers.

Recent advances in customizable HPC platforms, such as graphic processing unit (GPU) and field programmable gate array processor (FPGA) have brought significant progresses on communication-intensive tasks such as the Monte Carlo

---

[*]fumingw@xmu.edu.cn

simulations [43–47]. A FPGA-based computing system constructed by this group carried out Monte Carlo simulations of 1024×1024 Ising lattices at a speed of 10.6 picoseconds per spin update, a 1500x times speedup over an optimized CPU implementation [44]. The FPGA system has since been upgraded and Ising lattices up to 2048×2048 can be simulated now. The system can carryout Monte Carlo simulations at speeds up to 4.88 picoseconds per spin update, which is close to a 2.2 times speedup over the previous best FPGA system, a 26 times speedup over a single GPU and a 3300 times speedup over a single CPU. This spin update speed also breaks the previous record of 4.94 picoseconds per spin update achieved by a 64-GPU cluster [46]. The popular symmetric-multiprocessing-based (SMP) multiprocessor general purpose computers are expected to have similar speedup factors as the acceleration acquired from multithreading is mostly offset by less optimization in synchronized codes.

The longest single simulation consists of 1.7×10^{10} Monte Carlo sweeps (MCS) and runs for about 4.1 days on the upgraded FPGA device, which would need over 37 years of equivalent simulation time on a general purpose computer. The study has a total of over 3200 hours of simulation time on the FPGA systems, which is equivalent to over 1000 years of simulation time on a single general purpose computer. The steep computational cost makes accurate measurement of the linear relaxation time on general purpose computers impractical for lattice sizes greater than 512.

The paper is constructed as follows: Sec. II gives a brief description of the theoretical background; Sec. III introduces the FPGA system and the simulation parameters; Sec. IV presents the simulation data and their analysis; and Sec. V discusses implications of the obtained results.

II. LINEAR RELAXATION TIME

The dynamics of Ising models (model A) can be described by a purely dissipative stochastic Langevin equation with the Ginsburg-Landau Hamiltonian, also known as the time-dependent Ginsburg-Landau equation (TDGL) [48,49]

$$\frac{\partial \sigma(x,t)}{\partial t} = -\Omega \frac{\delta H[\sigma]}{\delta \sigma(x,t)} + \zeta(x,t)$$
$$\langle \zeta(x,t)\zeta(x',t') \rangle = 2\Omega\delta(x-x')\delta(t-t'), \tag{1}$$

where $\sigma(x,t)$ is an one-component continuous spin field, $H[\sigma]$ is the dimensionless Ginsburg-Landau Hamiltonian of the system, $\zeta(x,t)$ represents the Gaussian noise from the heat bath, and Ω is the dissipation constant. The corresponding Fokker-Planck equation for distribution of the spin field $P(\sigma,t)$ is

$$\frac{\partial P(\sigma,t)}{\partial t} = -H_{FP}P(\sigma,t), \tag{2}$$

where the operator H_{FP} is the Fokker–Planck Hamiltonian given by

$$H_{FP} = -\Omega \int d^d x \frac{\delta}{\delta\sigma(x)}\left[\frac{\delta H}{\delta\sigma(x)} + \frac{\delta}{\delta\sigma(x)}\right].$$

Equation (2) has a similar form as the Schrödinger equation, but operator H_{FP} is not Hermitian. A modified distribution $\tilde{P}(\sigma,t) = e^{-H/2}P(\sigma,t)$ can be defined to satisfy a similar equation

$$\frac{\partial \tilde{P}(\sigma,t)}{\partial t} = -\tilde{H}_{FP}\tilde{P}(\sigma,t), \tag{3}$$

where

$$\tilde{H}_{FP} = -\Omega\left(-\frac{\delta}{\delta\sigma(x)} + \frac{1}{2}\frac{\delta H}{\delta\sigma(x)}\right)\left(\frac{\delta}{\delta\sigma(x)} + \frac{1}{2}\frac{\delta H}{\delta\sigma(x)}\right)$$

is now a Hermitian operator. Solving Eq. (3), we will have a solution as

$$\tilde{P}(\sigma,t|\sigma_0) = \sum_{n=0}^{\infty} c_n(\sigma_0)e^{-\lambda_n t}\theta_n(\sigma), \tag{4}$$

where σ_0 is the initial spin field distribution, $\lambda_n \geqslant 0$ are the eigenvalues, and $\theta_n(\sigma)$ are the eigenvectors of Eq. (3). The ground state $(n = 0)$ corresponds to the equilibrium distribution of the system $(P_{eq}(\sigma) = e^{-H})$, while the excited states $(n > 0)$ give the thermal fluctuation modes. The time-delayed correlations between thermal fluctuations of the order parameter can then be expressed in terms of the excited states (modes) as

$$\langle M(t)M(0)\rangle = \sum_{\{\sigma,\sigma_0\}} M(\sigma,t)M(\sigma_0,0)P(\sigma,t|\sigma_0) = \sum_{j=1}^{\infty} a_j e^{-t/\tau_j}, \tag{5}$$

where M is the magnetization, $\tau_j = 1/\lambda_j$ is the relaxation time for the jth excited mode, and a_j are t independent constants.

For an infinite system with a temperature approaching the critical temperature T_c, τ_j diverges and causes the "critical slowing down" effect. According to the dynamic critical scaling hypothesis [48,50–52], the diverging relaxation times τ_j have a power-law relation to the diverging correlation length ξ, which is defined as $\xi \propto |T - T_c|^{-\nu}$. We define the exponent of this power-law relation as the dynamic exponent z and have the following relation

$$\tau_j \propto \xi^z. \tag{6}$$

As τ_j diverges, the relaxation process is dominated by the first excited mode. As a result, τ_1 becomes the relaxation time τ of the system, and Eq. (5) becomes

$$\langle M(t)M(0)\rangle \propto e^{-t/\tau}. \tag{7}$$

For finite systems at T_c, ξ goes to infinity and the relaxation process is dominated by the Fourier component of the excited modes that has the longest wavelength $\lambda_{max} \propto L$ or the smallest wave vector $k_{min} \propto L^{-1}$. The relaxation time of the system is then hypothesized to have a power law-relation with the λ_{max} or k_{min}. We now have

$$\tau_{FSS}(L) \propto L^z, \tag{8}$$

the FSS subscript is added to τ to distinguish it from simulated $\tau(L)$. Comparing to Eq. (6), we can see that the effective correlation length ξ in finite systems at T_c equals to the system size L. Combining Eqs. (7) and (8), one can calculate the relaxation times and the exponent z of finite Ising lattices from simulations of their linear relaxation processes.

For small finite systems, corrections to the FSS relations are needed. According to conformal invariance consideration

and the corresponding numerical results [53], the following corrected FSS relation can be used to study small Ising lattices

$$\tau_{\text{FSS}}(L) = L^z \sum_{k=0}^{n_c} b_k L^{-2k}, \qquad (9)$$

where b_k are constants and n_c limits number of the correction terms. This correction has been used in linear relaxation studies discussed earlier [24,25].

III. SIMULATE ISING MODELS WITH FPGA

FPGA is a new type of computing device that can generate user specific digital circuits in field, providing tremendous flexibility in architectural design and achieving astonishing performance improvements at certain computing tasks [54]. A high-end FPGA device can contain millions of logical elements (LEs), each of which can be programmed to carryout calculations concurrently, providing computational capabilities equivalent to tens of thousands of CPUs. Furthermore, the processing and the communicating of data in FPGA can be synchronized in pipelines to achieve very high efficiency, eliminating the "Von Neumann bottleneck" latency problem suffered by all CPU-based general purpose computers.

The METROPOLIS updating scheme is communication intensive, making it difficult and inefficient to implement them on clustering type of supercomputers. FPGA systems can be designed to carryout METROPOLIS updates very efficiently [43,44]. In this study, FPGA development boards including DE3 from Terasic® and DK-DEV-3CI20N from Altera® are used to implement the simulation systems. The FPGA chip on the DE3 board is a Stratix III (EP3SL340) from Altera®, which has 338k LEs and 18Mb Block RAM; the FPGA chip on the DK-DEV-3CI20N board is a Cyclone III (EP3C120) also from Altera®, which has 120k LEs and 4Mb Block RAM. The Cyclone III can only simulate Ising lattices no bigger than 1024×1024. It is used to ensure that simulation results are device independent. Both systems run at a 100-MHz system clock.

Circuitries for simulating 2D square Ising models with periodical boundaries are implemented using the VERILOG hardware description language (HDL) [44,55]. Processing units (PUs) are implemented to update Ising spins concurrently. A total of L PUs are implemented for a L x L Ising lattice, achieving linearly scaling simulation time over lattice size L. The speedup of the FPGA simulation system over general purpose computers increase with L, and the largest speedup close to 3300 times is achieved at $L = 2048$ in this study.

Nearest-neighbor METROPOLIS updating is implemented in each PU. The following VERILOG statement implements a PU that updates spin m according to its neighboring spin a, b, c, and d in the lattice

$$d <= ((m\hat{\ }a + m\hat{\ }b + m\hat{\ }c + m\hat{\ }d + R < p_1$$
$$+ R < p_2) < 2) ? \text{m} :\sim \text{m}. \qquad (10)$$

Here $\Leftarrow$ and $\hat{\ }$ are the nonblocking assignment and the XOR operators in VERILOG. R is the register that stores the pseudorandom number, and $p_1 = \exp(-4/T)$, $p_2 = \exp(-8/T)$ are registers that store the flipping probabilities. Temperature T is
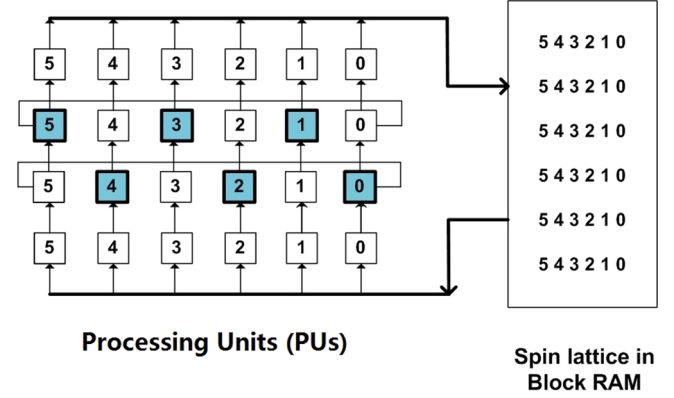

FIG. 1. Processing units (colored squares) that update nonneighboring spins concurrently. The arrows indicate the direction of the movements of the data after each updating operation.

set to the critical temperature T_c of the bulk 2D square Ising model. Notice that the updated value of spin m is assigned to the memory register occupied by neighboring spin d after the updating operation. In a similar fashion, every spin moves to one of their neighboring registers after each clock. A pipelining scheme shown in Fig. 1 is used so that only nonneighboring spins are updated concurrently at each clock. Details of the circuit designs have been reported elsewhere [44].

Random number generator (RNG) is an important part of any Monte Carlo simulation. Independent RNGs are allocated for each PU to parallelize the simulation process and to ensure their statistical independence. Implementations of high quality RNGs such as Mersenne twister [56] and WELL1024a [57] on FPGA are possible, but require too many resources. Instead, a 32-bit shift-register-type of RNG such as the linear feedback shift register (LFSR) and cellular automata shift register (CASR) are implemented to supply up to 6.6 THz high-quality random bits. LFSRs are constructed using primitive polynomials taken from [58] to ensure maximum length bit sequences. LFSR and CASR are combined via mod-2 addition (XOR) to obtain new sequences with a much longer period and better statistical quality [59–62]. A drawback of LFSR is that it can only produce one new bit from each update operation. One would need to either use random numbers with overlapping bit sequences or to carryout multiple update operations for each random number. Recently, Gu *et al.* developed a new type of FPGA-based LFSR called Leap LFSR, which can combine multiple update operations into a single one [63]. With Leap LFSR, one can obtain nonoverlapping random numbers using just one tick of the system clock.

Three types of 32 bit RNGs are implemented and tested in this study. RNG No. 1 is an 81 bit Leap LFSR with a period of $2^{81} - 1$ using primitive polynomial $x^{81} + x^{77} + 1$. RNG No. 2 is constructed via mod-2 addition (XOR) of a 52-bit Leap LFSR and a 37-bit CASR. Primitive polynomial $x^{52} + x^{49} + 1$ and CA rule 30 are used respectively and the period should be close to 2^{89} [34,44,58,61]. Finally, RNG No. 3 is the same type of RNG reported in [44], which is the mod-2 addition (XOR) of a 43-bit LFSR, a 37-bit CASR and a 1-bit true random source. The 43-bit LFSR in RNG No. 3 can only produce overlapping 32-bit random numbers, and the 37-bit CASR is the same as

in RNG No. 2. The true random bit is obtained by harvesting thermal jitters in the FPGA circuit and is updated at a minimum frequency of 3.1 KHz [44,64,65]. The period of RNG No. 3 is theoretically infinite due to the inclusion of a true random bit. Segments of the VERILOG programs that implement these RNGs are listed in the supplemental material [66].

It is found that all three types of RNGs generate high-quality pseudorandom numbers that pass the NIST random number testing suit with similar fail rates as high quality RNGs such as Mersenne twister and WELL1024a [44,56,57]. However, further tests have shown that only RNG No. 2 gives the correct static FSS behavior for large Ising lattices, while the other two types of RNGs show considerable deviations from the static scaling law (see Sec. IV).

To achieve high accuracy, Ising systems are simulated for a total simulation time greater than 1000τ. The system starts from a uniform spin orientation, and follows with a 300τ relaxation period to relax the system to an equilibrium state. After that, the magnetization of the system is recorded every 0.0005τ and about 2×10^6 samples are collected for each run. Data from RNG No. 1 have three simulation runs per data point while those from RNG Nos. 2 and 3 have five or more simulation runs per data point. The standard deviation of the mean of the runs at each data point is used for error estimation, which are then calculated from unbiased standard deviations of runs [67]. The errors in the results from linear regressions are estimated according to methods described in [62].

IV. SIMULATION RESULTS

Before analyzing the dynamic FSS behavior of the critical Ising lattices, we take a look at their static FSS behavior to verify the simulation system. The FSS behavior of static properties like isothermal susceptibility $\chi(L)$ is well understood [68], and can be calculated with a much higher accuracy. One can therefore verify the simulation system by comparing the observed FSS behavior to that of the static FSS theory.

According the static FSS theory, $\chi(L)$ should have the following scaling property

$$\chi(\varepsilon, L) = L^{\gamma/\nu}\chi^0(\varepsilon L^{1/\nu}), \tag{11}$$

where $\varepsilon = (T - T_c)/T_c$, and γ and ν are the critical exponents of bulk 2D Ising lattice. At T_c, $\varepsilon = 0$, and Eq. (11) becomes

$$\chi_{\mathrm{FSS}}(L) \propto L^{\gamma/\nu}. \tag{12}$$

The subscript FSS is added to distinguish it from simulated $\chi(L)$.

Ising lattices with sizes between 32 and 2048 are simulated with three types of RNGs. The susceptibilities $\chi(L)$ from these simulations are calculated from the second moment of the magnetization M. The log of $\chi(L)/\chi_{\mathrm{FSS}}(L)$ is plotted against the log of L in Fig. 2, where the proportional constant in Eq. (12) is determine by requiring $\chi_{\mathrm{FSS}}(32) = \chi(32)$. The correct FSS scaling behavior should produce data points identical to $\chi_{\mathrm{FSS}}(L)$, which is along the horizontal axis. We see that only data from RNG No. 2 (circles) show this behavior, while those from the other two RNGs show considerable deviations, indicating deficiencies in these RNGs. A linear regression is carried out between the logs of $\chi(L)$ and L from RNG No. 2, and a scaling exponent of 1.7498(4) is
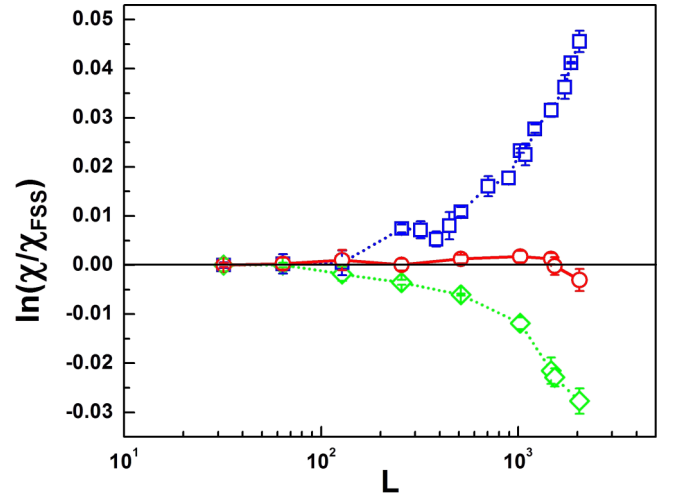

FIG. 2. The log of susceptibility χ over FSS theory $\chi_{\mathrm{FSS}}(L)$ from RNG No. 1 (diamonds), RNG No. 2 (circles), and RNG No. 3 (squares). The error bars are the standard deviations of the mean of the multiple runs at each point

obtained, which is very close to the theoretical value of 1.750. We therefore conclude that our simulation system with RNG No. 2 is sound.

The standard deviations of the mean are calculated from multiple runs at each data point for its error bar. We observe that the error bars are quite small compared to the displayed fluctuations of the data points, especially for RNG No. 1. This should be in part due to fluctuations caused by the limited number of runs, e.g., RNG No. 1 data have only three runs per data points, and in part due to the systematic errors introduced by correlations in the RNGs.

We now start to analyze the dynamic FSS behavior of the critical Ising lattices. A segment of the magnetization for a 2048×2048 Ising lattice at the critical temperature T_c is shown in Fig. 3. Frequent directional flips of the magnetization are observed as expected even for such a large lattice. The log of the autocorrelation $\langle M(t)M(0)\rangle/\langle M^2\rangle$ for
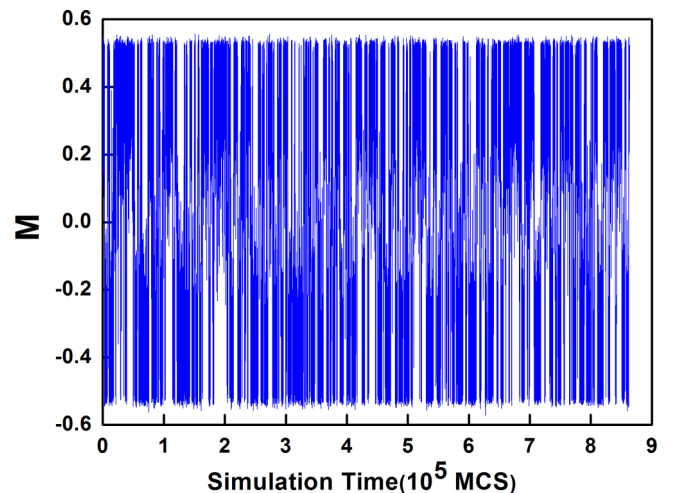

FIG. 3. Magnetization m of a 2048×2048 Ising lattice as a function of simulation time t.
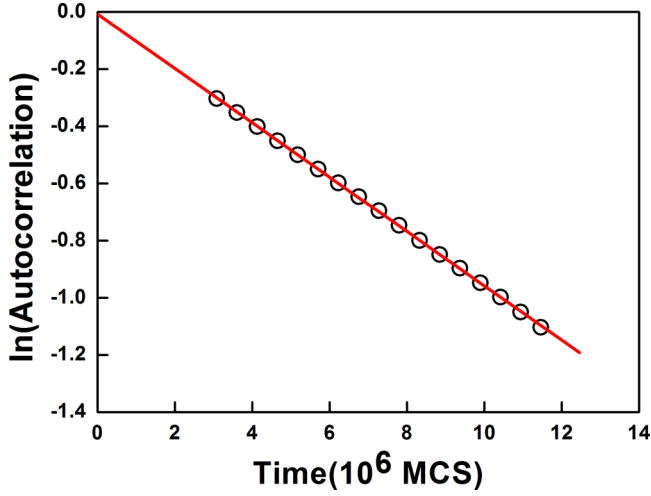
FIG. 4. The log of the autocorrelation of the magnetization in a 2048×2048 Ising lattice as a function of time delay t. The straight line is a linear fit to the data.

the Ising lattice is calculated and shown in Fig. 4. Due to the extremely long simulation time, the average magnetization $\langle M \rangle$ is very small and hence has been assigned to its theoretical value of zero for the autocorrelation calculations. Most autocorrelation data have excellent linearity as the one shown in Fig. 4. The relaxation time τ is calculated from a linear fit according to Eq. (7). The autocorrelation data are fitted between approximately 0.3τ and 1.1τ. This fitting range is selected to avoid the initial nonlinearity and to retain a good signal-to-noise ratio at the same time. Such an ideal choice is only possible with the high quality data generated from extremely long simulations.

Next, a log-log plot of relaxation time τ over size L is shown in Fig. 5, where the errors of the data points are less than the size of the symbols. A straight line is fitted to the data according Eq. (8), assuming correction terms shown in Eq. (9) can be neglected. Excellent agreement between theory and data is observed. The dynamic exponent $z = 2.179(12)$ is obtained from the slope of the straight line, which is very
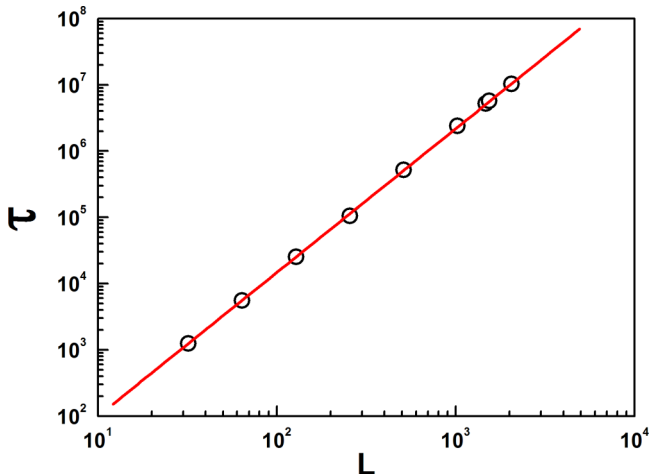

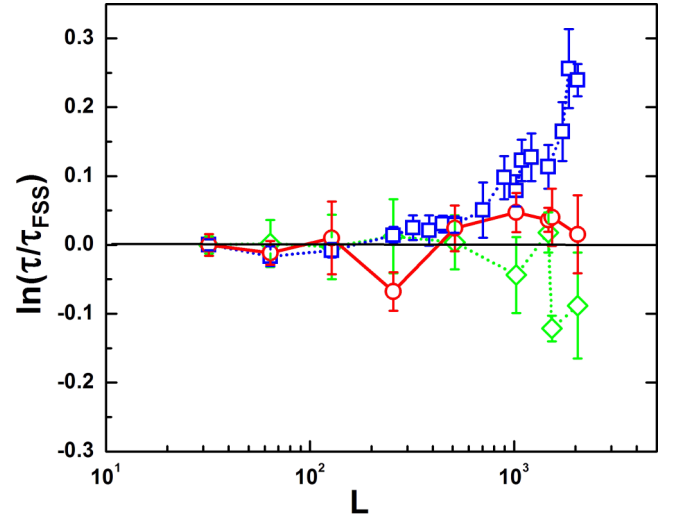FIG. 5. The log-log of relaxation time τ and lattice size L from RNG No. 3.

FIG. 6. The log of relaxation time τ over FSS theory $\tau_{FSS}(L)$ from RNG No. 1 (diamonds), RNG No. 2 (circles), and RNG No. 3 (squares). The error bars are the standard deviations of the mean of the multiple runs at each point.

close to the 2.167 value obtained by previous nonequilibrium and stochastic matrix studies. To compare the obtained τ to the dynamic FSS theory more closely, we plot $\log(\tau/\tau_{FSS})$ in Fig. 6. τ_{FSS} is calculated according to Eq. (8) where z is set to 2.167 and the proportional constant is determined by requiring τ_{FSS} equal to τ when $L = 32$. For comparison, data from RNG Nos. 1 and 3 are also included in the plot. The error bars are the standard deviations of the mean at each data point. We can see that the $\log(\tau/\tau_{FSS})$ data from RNG No. 2 (circles) stay close to the horizontal axis which represents the scaling behavior of τ_{FSS}, while those from the other two RNGs show noticeable deviations as L is increased past 512.

To investigate the possible effects of the correction terms in Eq. (9), we gradually remove the smaller lattices from the RNG No. 2 data to gradually reduce the effects of the correction terms. To make this analysis more effective, we remove the point at $L = 256$, which can easily be identified as an outlier. With this outlier, the following analysis produces large fluctuations. Linear regressions are carried out on these reduced data sets and the results are listed in Table I. We can see that the z values are quite stable as the smaller lattices are removed from the data. This means that the correction effects are not important and the linearity between $\log(\tau)$ and $\log(L)$

TABLE I. Linear regression of $\log(\tau)$ over $\log(L)$ for Ising lattices with different range of sizes. The maximum size is always 2048 while the minimum size is listed in the first column. The rest of the columns are the dynamic exponent z, its fitting error, and the reduced χ^2 of the fits. The outlier at $L = 256$ is removed during this analysis.

$L \geqslant$	z	Error	χ^2
32	2.177	0.009	0.22
64	2.179	0.012	0.16
128	2.176	0.018	0.16
512	2.165	0.036	0.21

is very good. The errors are increased due to the reduction of the number of data points.

Compared to Fig. 2, we see similar deviation patterns from the "poor" RNGs, except the effect is much larger scale in dynamic FSS. In both static and dynamic FSS, the effects of "poor" RNGs only become significant when the size of the Ising lattice is greater than 512. It also is interesting to note that the directions of the deviations from the "poor" RNGs are correlated in static and dynamic FSS, i.e., RNG No. 1 produces smaller χ and shorter τ while RNG No. 3 produces larger and longer ones. Apparently, the statistical correlations in RNGs can both decelerate and accelerate the critical relaxation process in 2D Ising systems.

In Fig. 6, we also notice that the error bars increase with L. This is due to the relative longer simulation times assigned to the smaller Ising lattices. In our study, a constant number of samples are collected for all runs and the sampling rate is calculated so that the total simulation time is 1000 times the relaxation time. The appropriate sampling rate for small lattices is smaller than the minimum possible sampling period of 1 MCS per sample, making the total simulation time relatively longer for these smaller lattices. This means that longer simulation time leads to smaller errors, which is in accordance with the previous understandings on this matter [44,69].

V. DISCUSSIONS

To answer the questions posed at the beginning of the paper: the dynamic exponent z remain the same for Ising systems with much longer correlation lengths. This result confirms Eq. (9) and the dynamic critical scaling hypothesis [50–52] for 2D Ising lattices up to 2048×2048. Combining results from [24], Eq. (9) has been verified for 2D Ising lattices ranging from 4×4 to 2048×2048, which is a much more extended test than any previous studies. This is also the first time that linear relaxation simulations give a consistent exponent z as the nonequilibrium and stochastic matrix studies.

Assuming a lattice constant of 1 nm, which is reasonable for a diluted ferromagnet, the largest Ising lattice simulated in this study corresponds to a $2 \times 2 \, \mu m^2$ ferromagnet, which is already in the macroscopic range. It seems that we have extended the test close to the macroscopic limit and one can conclude that the exponent z of all finite 2D Ising lattices is indeed around 2.167. On the other hand, the obtained exponent z does not agree with either the 2.50 value from the $1 + \varepsilon$ RG transformation study [32] or the 2.0 value from Domany's report [33], leaving some uncertainties on the issue. Recently in several studies, Schwartz and Edwards present theoretical evidences of slower than exponential decay of correlations in nonlinear systems including critical Ising lattices approaching infinite size [7,70,71]. This result suggests that deviations from the dynamic FSS theory may occur as the system size approaching infinity. Future dynamic FSS investigations may confirm such predictions.

From Figs. 2 and 6, we can see that the simulation of the critical processes in Ising lattices, especially of the dynamics critical processes, becomes sensitive to the statistical correlations in the RNGs as the lattice size becomes larger than 512. It seems that the statistical correlations in the RNGs

can both accelerate and decelerate the relaxation process, which in turn gives shorter and longer relaxation times for the system. It has long been suspected that statistical correlations which unavoidably exist in all RNGs would manifest themselves in larger systems and longer processes. Figures 2 and 6 demonstrate when and how such manifestation becomes significant. It also demonstrates that passages in the current random number test suites are not a proof of adequate randomness in the RNGs, at least not for critical dynamics studies; further tests such as static FSS tests are required. Understanding of the mechanisms behind these behaviors may gain us insights on both the random number generation and the critical relaxation processes.

The observed bias amplification effect makes the investigation of larger Ising lattices even more difficult, as a RNG with even "higher" quality and more logical resources may be required to produce consistent simulation results. It would be interesting to find out in the future when and how high quality RNGs such as Mersenne twister and WELL1024a give noticeable deviations in large critical Ising lattices.

Shchur and Blöte studied the bias effects of LFSR-type RNGs on the calculation of static properties such as energy and specific heat of critical Ising lattices [72]. They found that the bias reaches a maximum and decreases as the lattice size increases further. This behavior was explained by the relative bit shifting patterns in their LFSR RNGs. We do not see such a behavior in this study because our random numbers are either a combination of two RNGs or do not have overlapping bit sequences so that no relative bit-shifting patterns exists in consecutive random numbers.

Our FPGA-based simulation system allows us to test both the static and the dynamic critical FSS behavior in larger systems and longer periods that are unreachable before, and the continued progress of the FPGA technology will enable us to explore even larger systems and longer periods in the future. The platform can easily be adapted for studying of similar systems such as spin glass and random bond or random site Ising models, which also display interesting long time behaviors.

VI. CONCLUSION

Nearest-neighbor square Ising lattices with periodical boundaries sizing from 32×32 up to 2048×2048 are studied on FPGA-based computing devices. The linear relaxation processes in these lattices are simulated at the bulk critical temperature for extremely long durations to obtain accurate evaluations of their linear relaxation times.

It is found that the linear relaxation time scales with the power of the lattice size in accordance with the dynamic FSS theory for correlation lengths as long as 2048. The dynamic exponent z is determined to be 2.179(12), which is consistent with the previous nonequilibrium and stochastic matrix studies of Ising systems with much shorter correlation lengths.

It is noticed that simulations of critical dynamics in Ising lattices become sensitive to the statistical correlations between pseudorandom numbers when the lattices size is larger than 512, and this effect makes the investigation of critical dynamics in larger Ising lattices even more difficult.

[1] K. G. Wilson, Rev. Mod. Phys. **55**, 583 (1983).

[2] K. Nam, B. Kim, and S. J. Lee, Phys. Rev. E **77**, 056104 (2008).

[3] X. Huang, S. Gong, F. Zhong, and S. Fan, Phys. Rev. E **81**, 041139 (2010).

[4] M. Y. Nalimov, V. A. Sergeev, and L. Sladkoff, Theor. Math. Phys. **159**, 499 (2009).

[5] A. S. Krinitsyn, V. V. Prudnikov, and P. V. Prudnikov, Theor. Math. Phys. **147**, 561 (2006).

[6] M. J. Dunlavy and D. Venus, Phys. Rev. B **71**, 144406 (2005).

[7] M. Schwartz and S. F. Edwards, Europhys. Lett. **56**, 499 (2001).

[8] M. Schwartz, J. Phys. A: Math. Gen. **36**, 7507 (2003).

[9] E. Lubetzky and A. Sly, Commun. Math. Phys. **313**, 815 (2012).

[10] H. C. Bolton and C. H. J. Johnson, Phys. Rev. B **13**, 3025 (1976).

[11] J. K. Williams, J. Phys. A: Math. Gen. **18**, 49 (1985).

[12] S. Tang and D. P. Landau, Phys. Rev. B **36**, 567 (1987).

[13] N. Ito, M. Taiji, and M. Suzuki, J. Phys. Soc. Jpn. **56**, 4218 (1987).

[14] J. S. Wang and C. K. Gan, Phys. Rev. E **57**, 6548 (1998).

[15] H. K. Janssen, B. Schaub, and B. Schmittmann, Z. Phys. B **73**, 539 (1989).

[16] D. Stauffer, Physica A **184**, 201 (1992).

[17] N. Ito, Physica A **192**, 604 (1993).

[18] H. W. Diehl and U. Ritschel, J. Stat. Phys. **73**, 1 (1993).

[19] A. Linke, D. W. Heermann, and P. Altevogt, Comput. Phys. Commun. **90**, 66 (1995).

[20] Z. Li, L. Schülke, and B. Zheng, Phys. Rev. E **53**, 2940 (1996).

[21] F. G. Wang and C. K. Hu, Phys. Rev. E **56**, 2310 (1997).

[22] M. Silvério Soares, J. K. da Silva, and F. C. SáBarreto, Phys. Rev. B **55**, 1021 (1997).

[23] B. Zheng, Physica A **283**, 80 (2000).

[24] M. P. Nightingale and H. W. J. Blöte, Phys. Rev. Lett. **76**, 4548 (1996).

[25] M. P. Nightingale and H. W. J. Blöte, Phys. Rev. B **62**, 1089 (2000).

[26] Z. Racz and M. F. Collins, Phys. Rev. B **13**, 3074 (1976).

[27] B. Damman and J. D. Reger, Europhys. Lett. **21**, 157 (1993).

[28] J. Wang, Phys. Rev. B **47**, 869 (1993).

[29] K. G. Wilson and M. E. Fisher, Phys. Rev. Lett. **28**, 240 (1972).

[30] B. I. Halperin, P. C. Hohenberg, and S. Ma, Phys. Rev. Lett. **29**, 1548 (1972).

[31] C. D. Dominicis, E. Brézin, and J. Zinn-Justin, Phys. Rev. B **12**, 4945 (1975).

[32] R. Bausch, V. Dohm, H. K. Janssen, and R. K. P. Zia, Phys. Rev. Lett. **47**, 1837 (1981).

[33] E. Domany, Phys. Rev. Lett. **52**, 871 (1984).

[34] S. Wolfram, Rev. Mod. Phys. **55**, 601 (1983).

[35] Y. C. Kim, M. A. Anisimov, J. V. Sengers, and E. Luijten, J. Stat. Phys. **110**, 591 (2003).

[36] R. M. K. Tsiaze, S. E. M. Tchouobiap, J. E. Danga, S. Domngang, and M. N. Hounkonnou, J. Phys. A: Math. Theor. **44**, 285002 (2011).

[37] J. V. Sengers and J. G. Shanks, J. Stat. Phys. **137**, 857 (2009).

[38] S. Wansleben and D. P. Landau, J. Appl. Phys. **61**, 3968 (1987).

[39] N. Ito, M. Taiji, and M. Suzuki, J. Phys. Colloques **49**, C8-1397-98 (1988).

[40] M. Mori and Y. Tsuda, Phys. Rev. B **37**, 5444 (1988).

[41] A. M. Ferrenberg and D. P. Landau, Phys. Rev. B **44**, 5081 (1991).

[42] J. Backus, Commun. ACM **21**, 613 (1978).

[43] F. Belletti *et al.*., Comput. Phys. Commun. **178**, 208 (2008).

[44] Y. Lin, F. Wang, X. Zheng, H. Gao, and L. Zhang, J. Comput. Phys. **237**, 224 (2013).

[45] T. Preis, P. Virnau, W. Paul, and J. J. Schneider, J. Comput. Phys. **228**, 4468 (2009).

[46] B. Block, P. Virnau, and T. Preis, Comput. Phys. Commun. **181**, 1549 (2010).

[47] M. Weigel, J. Comput. Phys. **231**, 3064 (2012).

[48] S. Ma, *Modern Theory of Critical Phenomena* (Westview, Boulder, CO, 1976).

[49] J. Zinn-Justin, *Quantum Field Theory and Critical Phenomena* (Clarendon, New York, 1989).

[50] B. I. Halperin and P. C. Hohenberg, Phys. Rev. **177**, 952 (1969).

[51] P. C. Hohenberg and B. I. Halperin, Rev. Mod. Phys. **49**, 435 (1977).

[52] M. Suzuki, Prog. Theor. Phys. **58**, 1142 (1977).

[53] H. W. J. Blöte and M. P. M. den Nijs, Phys. Rev. B **37**, 1766 (1988).

[54] M. C. Herbordt *et al.*., Computer **40**, 50 (2007).

[55] D. E. Thomas and P. R. Moorby, *The Verilog Hardware Description Language* (Kluwer, Norwell, MA, 2002).

[56] M. Matsumoto and Y. Kurita, ACM Trans. Model. Comput. Simul. **4**, 254 (1994).

[57] F. O. Panneton, P. L'Ecuyer, and M. Matsumoto, ACM. Trans. Math. Softw. **32**, 1 (2006).

[58] P. Alfke, Xilinx Application Note XAPP 052 (1996).

[59] P. L'Ecuyer, Commun. ACM **31**, 742 (1988).

[60] A. Compagner, J. Stat. Phys. **63**, 883 (1991).

[61] T. E. Tkacik, Lect. Notes Comput. Sc. **2523**, 450 (2002).

[62] W. H. Press, S. A. Teukolsky, W. T. Vetterling, and B. P. Flannery, *Numerical Recipes: The Art of Scientific Computing*, 3rd ed. (Cambridge University Press, New York, 2007).

[63] X. Gu and M. Zhang, *International Conference on Computer and Communications Security (ICCCS), Hong Kong*, Vol. 150 (IEEE, Piscataway, 2009).

[64] R. J. Zhang, China Integr. Circuit **17**, 52 (2008).

[65] J.-L. Danger, S. Guilley, and P. Hoogvorst, Microelectron. J. **40**, 1650 (2009).

[66] See Supplemental Material at http://link.aps.org/supplemental/10.1103/PhysRevE.93.022113 for programs that implement the random number generators.

[67] B. W. Bolch, Am. Stat. **22**(3), 27 (1968).

[68] M. E. Fisher, in *Critical Phenomena, International School of Physics "Enrico Fermi,"* edited by M. S. Green (Academic, New York, 1971).

[69] A. M. Ferrenberg, D. P. Landau, and K. Binder, J. Stat. Phys. **63**, 867 (1991).

[70] S. F. Edwards and M. Schwartz, Physica A **303**, 357 (2002).

[71] M. Schwartz, Physica A **389**, 689 (2010).

[72] L. N. Shchur and H. W. J. Blöte, Phys. Rev. E **55**, R4905 (1997).